



# One-step CRISPR/Cas9 method for the rapid generation of human antibody heavy chain knock-in mice

Ying-Cing Lin<sup>1,†</sup>, Simone Pecetta<sup>1,†</sup>, Jon M Steichen<sup>2</sup>, Sven Kratochvil<sup>1</sup>, Eleonora Melzi<sup>1</sup> , Johan Arnold<sup>1</sup>, Stephanie K Dougan<sup>3</sup>, Lin Wu<sup>4</sup>, Kathrin H Kirsch<sup>1</sup>, Usha Nair<sup>1</sup>, William R Schief<sup>1,2</sup> & Facundo D Batista<sup>1,\*</sup> 

## Abstract

Here, we describe a one-step, *in vivo* CRISPR/Cas9 nuclease-mediated strategy to generate knock-in mice. We produced knock-in (KI) mice wherein a 1.9-kb DNA fragment bearing a pre-arranged human B-cell receptor heavy chain was recombined into the native murine immunoglobulin locus. Our methodology relies on Cas9 nuclease-induced double-stranded breaks directed by two sgRNAs to occur within the specific target locus of fertilized oocytes. These double-stranded breaks are subsequently repaired via homology-directed repair by a plasmid-borne template containing the pre-arranged human immunoglobulin heavy chain. To validate our knock-in mouse model, we examined the expression of the KI immunoglobulin heavy chains by following B-cell development and performing single B-cell receptor sequencing. We optimized this strategy to generate immunoglobulin KI mice in a short amount of time with a high frequency of homologous recombination (30–50%). In the future, we envision that such knock-in mice will provide much needed vaccination models to evaluate immunoresponses against immunogens specific for various infectious diseases.

**Keywords** antibody responses; B cells; bnAbs; CRISPR; knock-in

**Subject Categories** Genetics, Gene Therapy & Genetic Disease; Immunology

**DOI** 10.15252/embj.201899243 | Received 14 February 2018 | Revised 26 June

2018 | Accepted 5 July 2018 | Published online 7 August 2018

**The EMBO Journal (2018) 37: e99243**

## Introduction

B lymphocytes are central to humoral immunity because of their ability to produce antibodies in response to infection and immunization. Antibodies not only confer protection from infections, but also

represent the basis of most of the currently licensed human vaccines. Despite the great importance of antibodies for public health, the precise molecular mechanisms that drive their specificity, affinity, class switching, and durability are still under investigation. A more detailed understanding of the cellular and molecular mechanisms that drive B-cell function is critical for the development of treatments for B-cell dyscrasias and autoimmune diseases, and for the advancement of next-generation vaccines, particularly against challenging targets such as influenza and HIV (Pappas *et al*, 2014; Dosenovic *et al*, 2015; Jardine *et al*, 2015; Sanders *et al*, 2015; Briney *et al*, 2016; Escolano *et al*, 2016; Joyce *et al*, 2016; Kallewaard *et al*, 2016; Lee *et al*, 2016; Tian *et al*, 2016).

Antigen binding to pre-clustered B-cell receptors (BCRs) on the B-cell membrane triggers a complex signaling cascade leading to B-cell activation. This includes extensive reorganization of the actin cytoskeleton, which is involved in BCR signaling-induced Ca<sup>2+</sup> flux (Lanzavecchia, 1985; Wienands *et al*, 1996; Aman & Ravichandran, 2000; Batista & Neuberger, 2000; Hao & August, 2005; Lillemeier *et al*, 2006; Pierce & Liu, 2010; Treanor *et al*, 2010, 2011; Yang & Reth, 2010; Mattila *et al*, 2013; Tolar & Spillane, 2014; Spillane & Tolar, 2017). These events are followed by antigen internalization and endosomal trafficking, both of which are pre-requisites for antigen presentation to T cells, which drives the development of naïve B cells to germinal centers (GC) and differentiation into long-lived memory B cells (MBCs) and plasma cells (PCs) (Dal Porto *et al*, 2002; Shih *et al*, 2002; Okada *et al*, 2005; O'Connor *et al*, 2006; Paus *et al*, 2006; Qi *et al*, 2008; Gatto *et al*, 2009; Pereira *et al*, 2009; Schwickert *et al*, 2011; Taylor *et al*, 2012).

In the past, mouse models expressing pre-arranged BCRs having defined specificity for particular model antigens have proven to be extremely valuable in studying different aspects of B-cell function. This was initially accomplished by expressing BCRs at non-native loci. Indeed, the studies of such mice have been extremely valuable in advancing our knowledge of concepts such as B-cell tolerance

1 Ragon Institute of MGH, MIT and Harvard, Cambridge, MA, USA

2 Department of Immunology and Microbial Science and IAVI Neutralizing Antibody Center, The Scripps Research Institute, La Jolla, CA, USA

3 Dana-Farber Cancer Institute, Boston, MA, USA

4 Genome Modification Facility, Department of Molecular and Cellular Biology, Harvard University, Cambridge, MA, USA

\*Corresponding author. Tel: +1 857 268 7071; E-mail: fbatista1@mgh.harvard.edu

†These authors contributed equally to this work

and allelic exclusion (Goodnow *et al*, 1988, 1989). More recently, knock-in (KI) mouse models expressing pre-arranged BCRs at their native loci have been generated (Verkoczy *et al*, 2017). These animal models have been instrumental in furthering our understanding of fundamental B-cell attributes such as negative selection, receptor editing, anergy, class switch recombination, and somatic hypermutation, which were not possible to study when BCRs were recombined at random sites in the genome (Taki *et al*, 1993; Pelanda *et al*, 1997). However, all the BCR KI models described thus far have been generated by using gene modification in embryonic stem (ES) cells or by somatic cell nuclear transfer (SCNT) (Dougan *et al*, 2012). A major drawback of these methods is the long time required to generate a BCR KI mouse or highly specialized technical skills and equipment needed in the case of SCNT. The ES gene modification approach not only requires the generation of correct ES clones, but also all of the founder mice produced by this method are chimeras. These chimeric founders require further crossing for the complete germline transmission of insertions or deletions in order to obtain a stable line.

To alleviate this hurdle, we have developed a rapid one-step CRISPR/Cas9 nuclease-mediated KI strategy. In this method, Cas9 nuclease is directed by two guide RNAs to introduce double-stranded breaks within specific regions of the native murine immunoglobulin heavy chain locus of fertilized oocytes. Subsequently, large DNA fragments comprising pre-arranged immunoglobulin heavy (IgH) chains serve as templates for HDR giving rise to BCR KI mice within a matter of weeks rather than months. While the CRISPR/Cas9 technology is routinely used to generate mice bearing gene deletions and targeted insertions of short DNA fragments, our method allows for the rapid and reliable generation of KI mice with large DNA insertions, which was hitherto considered a challenge (Verkoczy *et al*, 2017). Using our methodology, we have generated and validated two such human IgH KI mouse models, which we report here. These KI mouse models express Ig V(D)J sequences encoding predicted germline sequences of HIV-1 broadly neutralizing antibodies (bnAbs) specific for the HIV-1 envelope V3 loop and surrounding spike glycans, PGT121, and BG18 (Julien *et al*, 2013; Freund *et al*, 2017). We envision that KI mouse models bearing specific immunoglobulin heavy or light chains will be valuable tools in testing the efficacy of particular immunogens in eliciting desired immune responses. As such, they offer the potential to drive vaccine development against HIV and other infectious diseases.

## Results

### One-step CRISPR generation of KI mice expressing human heavy chain

Our goal was to generate KI mice in a rapid and reproducible manner. To this end, we designed a strategy that relies on Cas9 nuclease to introduce double-stranded breaks specifically at the D<sub>4</sub>-J<sub>4</sub> region of the native IgH locus of fertilized oocytes (Fig 1A). The introduction of double-stranded DNA breaks can be repaired by either NHEJ or HDR (Maruyama *et al*, 2015). To drive integration of PGT121 via HDR in addition to the concomitant deletion of the native, murine D-J region, we introduced double-stranded breaks

using not one, but two sgRNAs. As the substrate of homologous repair, we generated a donor plasmid bearing 5' (3.9 kb) and 3' (2.6 kb) homology arms, a mouse VHJ558 promoter and leader region (1.5 kb), and a pre-assembled BCR (0.4 kb) expressing PGT121-gH (hereafter referred to as PGT121 for simplicity), the predicted germline VDJ sequence of the heavy chain of a monoclonal antibody, PGT121 (Fig 1A and B; described in Materials and Methods). This sequence, previously described as PGT121 GL<sub>CDR3rev1</sub>, has been fully germline-reverted except at two positions in the D gene (Steichen *et al*, 2016), and differs at eight CDR3 positions from the less-reverted sequence (PGT121<sub>CDR3rev4</sub>) used in a previously described PGT121 germline-reverted heavy chain KI mouse (Fig EV1) (Escolano *et al*, 2016; Steichen *et al*, 2016).

The specificity of CRISPR/Cas9-mediated genome editing is dependent on the sgRNA. Accordingly, we used the CRISPR DESIGN database (<http://crispr.mit.edu/>) to identify potential candidate protospacers, including 20 nucleotides complementary to the target sequence upstream of a protospacer adjacent motif (PAM) sequence (NGG). To avoid the cleavage of the homologous recombination arms of the DNA donor by Cas9 upon oocyte injection, we designed sgRNAs that only target sequences within the wild-type IgH locus but are not present within the homology arms of our donor plasmid. In an attempt to select for highly specific sgRNAs, which can potentially render this process more efficient in the mouse embryo, we first designed and examined the ability of 11 different sgRNAs to cleave a PCR amplicon containing the wild-type genomic DNA target in an *in vitro* assay (Appendix Table S1). As shown in Fig 1C, we identified three sgRNAs (sgRNAs 1, 4, and 6) that guide Cas9 to cleave the genomic DNA target around the D<sub>4</sub> region and three other guide RNAs (sgRNAs 7, 8, and 10) capable of targeting Cas9 to the J<sub>1-4</sub> regions. We chose sgRNA1 and sgRNA8 because they appeared to be the two most efficient candidates and confirmed that they did not exhibit any off-target effects on three selected amplicons from unrelated genes (Fig 1D and Appendix Table S2). After the injection of the two sgRNAs, Cas9 protein and plasmid DNA containing PGT121 germline sequence into fertilized oocytes, and subsequent implantation into pseudopregnant females, we obtained F0 founder mice potentially carrying our KI heavy chain.

As a first step to ascertain which of these founder mice is carrying the PGT121 insertion, we designed a screening protocol with three, independent TaqMan probes for genotyping. The first probe, Ighm-1 WT, is targeted to the WT C57Bl/6 mouse IgH D<sub>4</sub>-J<sub>1-4</sub> region; testing positive for this probe indicates that the WT locus is intact (WT mouse). The second probe, HulghV-4 Tg, is directed to the introduced PGT121 sequence and detects the integration of our PGT121 DNA. The third probe, KI-P, is targeted to the junction region between the 5' arm and VHJ558 promoter, and testing positive to this probe indicates the correct site of insertion of our PGT121 DNA (Figs 2A and EV2A).

In our initial experiment, after microinjecting 400 fertilized oocytes with sgRNA, Cas9 protein, and plasmid DNA containing PGT121 germline sequence and subsequently implanting them into pseudopregnant females, 15 pups were born. As determined from our screening protocol, out of these 15 pups, we found eleven founders that carried no deletions or insertions (WT<sup>+/+</sup>), three founders that carried deletions of the D<sub>4</sub> to J<sub>1-4</sub> segment in both alleles with no insertion of PGT121 (WT<sup>-/-</sup>), and lastly one founder in which the D<sub>4</sub> to J segment was replaced with a monoallelic insertion of

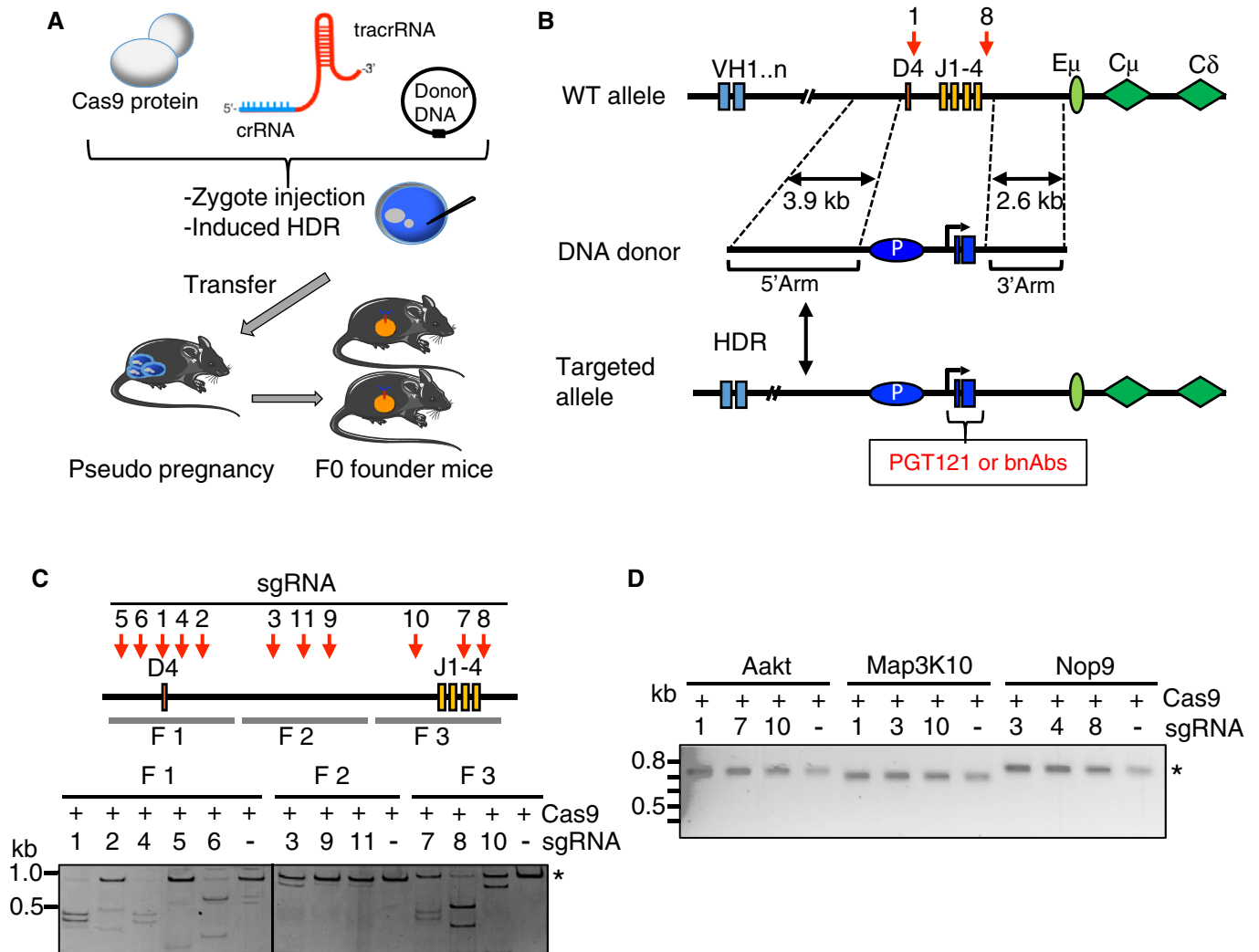


**Figure 1. One-step CRISPR zygote injection to generate mice carrying PGT121 heavy chain in the mouse IgH locus.**

**A** Schematic depicting CRISPR/Cas9 injection. A circular plasmid bearing germline PGT121-gH VDJ sequences, two guide RNAs, and Cas9 protein were injected into zygotes and implanted into pseudopregnant mice. Cas9-induced double-stranded breaks in the genome of zygotes are used to insert germline PGT121 VDJ sequences flanked by homologous arms on each side of the cut site via HDR. After 3 weeks, F0 founder mice are born, some of which bear the human bnAbs germline precursor.

**B** Strategy for insertion of PGT121 rearranged VDJ into mouse IgH locus. Targeting DNA donor with 5' (3.9 kb) and 3' (2.6 kb) homology arms to the C57BL/6 WT mouse IgH locus, murine VHJ558 promoter, leader, and the human PGT121 heavy chain VDJ sequences are located between two homology arms. CRISPR/Cas9-mediated HDR leads to the insertion of the promoter and PGT121 sequences into the C57BL/6 mouse genome. P: murine VHJ558 promoter; HDR: homology-directed repair; bnAbs: broadly neutralizing antibodies.

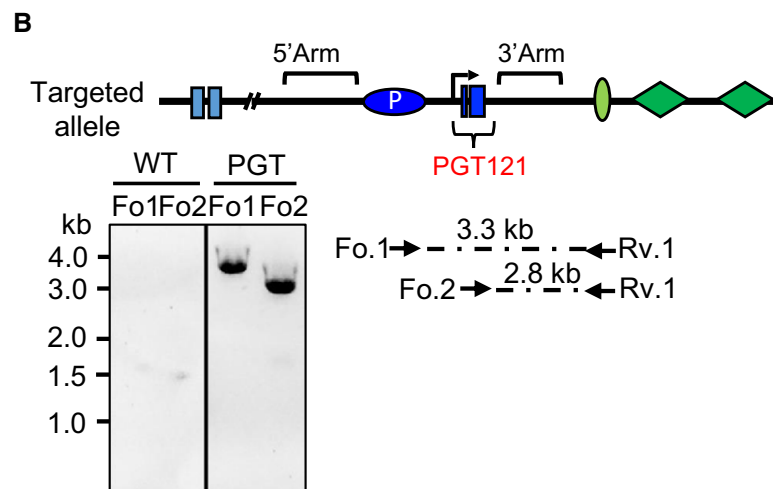
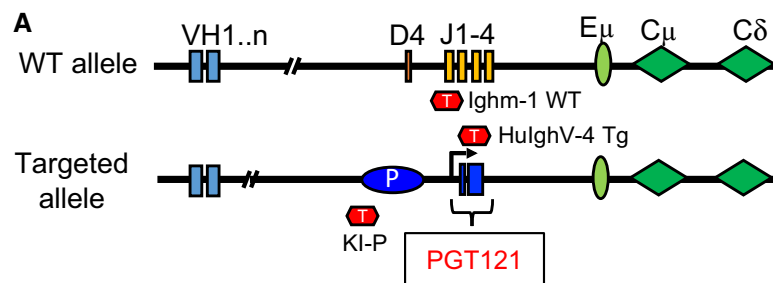
**C** sgRNA targeting sites are indicated in red. Three distinct fragments of genomic DNA were amplified by PCR, and *in vitro* digestion assay was performed with each of the sgRNAs to validate the efficiency of Cas9-mediated cleavage.

**D** Analysis sgRNA off-target effects in unrelated genes. Amplicons corresponding to Aakt, Map3K10, and Nop9 were generated by PCR by using gene-specific primers. *In vitro* digestion assay was performed to measure the Cas9-directed cleavage efficiency.

PGT121 (PGT121<sup>+/WT</sup>; Figs 2C and EV2B). Taken together, we observed that Cas9-driven deletion occurred at 26.7%, while the frequency of homologous recombination was only 6.7%. To validate whether the inserted IgH germline sequence (PGT121) was at the right genomic locus, we performed long-range PCR in the PGT121 mouse by amplifying the genomic DNA fragments using specific primers (Appendix Table S3). The two forward primers, Fo.1F and Fo.2F, were targeted at the promoter and PGT121 regions, respectively, and the reverse primer, Re.1R, was targeted at the region after the homologous 3' arm. We found amplicons of the correct size

only from genomic DNA amplified from the PGT121 KI mice, but not from WT mice, indicating that the PGT121 fragment had been inserted in the correct genomic locus (Fig 2B).

We performed another CRISPR injection (200 fertilized oocytes) with short arms (3.9 kb) of plasmid DNA and we observed that the frequency of Cas9-driven D<sub>4</sub>-J<sub>1-4</sub> deletion was 35.7%, while the frequency of homologous recombination was 0% (Fig 2C). We hypothesized that the low efficiency of HDR was likely to be a result of our relatively short homology arms. Accordingly, to increase the efficiency of this process, we extended each of the homology arms



**C**

CRISPR injection	5' Arm (kb)	3' Arm (kb)	# of HDR occurrence	Frequency (%)	# of Cas9-mediated D <sub>4</sub> -J <sub>4</sub> deletions	Frequency (%)	HIV bnAbs
1	3.9	2.6	1 of 15	6.7	4 of 15	26.7	HC1
2	3.9	2.6	0 of 14	0.0	5 of 14	35.7	HC2
3	5.0	5.0	16 of 50	32.0	17 of 50	34.0	HC1
4	5.0	5.0	10 of 49	20.4	13 of 49	26.5	HC2
5	5.0	5.0	16 of 33	48.5	18 of 33	54.5	HC3
6	5.0	5.0	7 of 14	50.0	7 of 14	50.0	HC4

**Figure 2. Characterization of PGT121 KI mice.**

A Schematic of the TaqMan probes and their targeting sites within the WT IgH and PGT121 IgH. T: TaqMan probe.  
 B Schematic showing the annealing sites of primers used to validate PGT121 KI animals. Fo.1F and Fo.2F primers were targeted at promoter region and PGT121 region, respectively, and combined with Re.1R primer targeted to the genomic region after homologous 3' Arm. KI alleles are predicted to result in the amplification of a Fo.1 fragment (3.3 kb) and Fo.2 fragment (2.8 kb). Genomic DNA was extracted from the F0 founders born after CRISPR injection or from a C57BL/6 (WT) mouse. Long-range PCR was performed to detect the insertion of the PGT121 VDJ sequences at the correct genomic locus.  
 C Table showing the frequency of the different genotypes of mice generated after CRISPR injection with plasmid donors containing long or short homology arms. # of HDR occurrence indicates the integration of the PGT121 heavy chain in the mouse IgH locus. # of Cas9-mediated D<sub>4</sub>-J<sub>4</sub> deletions indicates the efficiency of our sgRNA-directed Cas9 double-stranded breaks. HC: heavy chain.

to 5 kb (Fig EV3). This enhancement in arm length coincided with an increase in HDR observed in the founders. Indeed, 50 pups were born following the injection of this plasmid, among which there were 14 PGT121<sup>+/WT</sup> mice, one PGT121<sup>+/-</sup> mouse, and one

WT<sup>-/-</sup> and 34 WT<sup>+/+</sup> mice. It appears that the extended homology arms increased our HDR efficiency to 30%, while the rate of deletion remained constant (32%). This higher rate of recombination was confirmed by performing three independent injections, from

which the average frequency of HDR reached 40% with a similar rate of genomic DNA cleavage (Fig 2C).

We further crossed several of our positive heavy chain KI F0 founders with WT mice and followed the frequency of germline transmission of the KI heavy chain. Six out of 10 F0 mice revealed the Mendelian transmission of the heavy chain, while three out of ten F0 founders exhibited non-Mendelian transmission, indicating likely mosaicism, and one of our founders most likely has more than one insertion of our KI heavy chain (Fig EV4).

Collectively, our results demonstrate that we can reliably generate heavy chain KI mice *in vivo* by CRISPR/Cas9 within a short period of few weeks. This represents a significant step forward towards the rapid and reproducible generation of IgH KI mice.

### Characterization of B lymphocytes in the PGT121 KI mouse

To examine the impact of PGT121 germline heavy chain insertion on B-lymphocyte development, we analyzed the bone marrow progenitors of 8- to 10-week-old WT and PGT121<sup>+/WT</sup> mice by flow cytometry, using the Hardy classification system (Hardy *et al*, 1991). When compared to WT mice, we observed a similar frequency of immature, defined as early (B220<sup>+</sup>CD43<sup>+</sup>) and late (B220<sup>+</sup>CD43<sup>-</sup>), B cells in the bone marrow of PGT121<sup>+/WT</sup> mice (Fig 3A). However, when we examined the B cell subpopulations in the early immature compartment, we observed a significant reduction in the (CD24<sup>+</sup>BP-1<sup>+</sup>) B cell fraction C (Fig 3B). In contrast, the late immature B cell subpopulations from the bone marrow were not affected (Fig 3C). These results suggested that the expression of the PGT121 germline heavy chain might compromise the ability of KI B cells to pass tolerance checkpoints in the bone marrow (positive selection, stage C), possibly leading to the elimination or BCR editing of these cells.

To further characterize the progression of transitional B cells toward mature B lymphocytes, we analyzed peripheral B cells from blood, spleen, and peritoneal cavity by flow cytometry. Consistent with defects we observed in the bone marrow, we found a significant diminution in the number of B cells in the blood (Fig 4A). In contrast, we observed comparable numbers of B and T cells between these KI and WT mice, indicating that spleen cellularity was largely unaltered in PGT121<sup>+/WT</sup> mice (Fig 4B and C). However, we noticed a slightly decreased proportion of T1 cells (CD21<sup>lo</sup>CD24<sup>hi</sup>) within the B220<sup>+</sup> B-cell compartment. Furthermore, PGT121<sup>+/WT</sup> B cells retained their maturation potential, as we found similar amounts of both mature follicular (CD21<sup>hi</sup>CD24<sup>lo</sup>), marginal zone B cells (CD21<sup>hi</sup>CD24<sup>hi</sup>CD23<sup>-</sup>), and T2 cells (CD21<sup>hi</sup>CD24<sup>hi</sup>CD23<sup>+</sup>) in WT and PGT121<sup>+/WT</sup> mice (Fig 4D and E). We also analyzed the lymphocyte populations in the peritoneal cavity of these animals. Here, we observed that WT and PGT121<sup>+/WT</sup> mice had comparable numbers of B2 (CD5<sup>-</sup>CD11b<sup>-</sup>) and B1a (CD5<sup>+</sup>CD11b<sup>+</sup>) but a slight diminution of B1b (CD5<sup>-</sup>CD11b<sup>+</sup>) cells (Fig 4F). Together, these results suggest that the establishment of mature lymphocyte populations is not affected in the PGT121<sup>+/WT</sup> mouse.

To understand whether the histological organization of lymphoid organs was altered in the PGT121 KI mouse line, we assessed the anatomical structure of the spleen by confocal microscopy. We observed a normal compartmentalization of the splenic tissue, comprised of white pulp and red pulp area in normal proportion,

the latter populated by F4/80<sup>+</sup> macrophages (Fig 4G). The cellular localization appeared normal in the white pulp, with central T cells (TCR $\beta$ ) surrounded by B cell (B220<sup>+</sup>) organized into follicles delimited by metallophilic marginal zone macrophages (CD169<sup>+</sup>). Inside the follicles, B cells presented a normal phenotype and we could identify follicular B cell (CD23<sup>high</sup>IgM<sup>low</sup>) and marginal zone B cell (CD23<sup>-</sup>IgM<sup>+</sup>) separated by a thin line of CD169<sup>+</sup> macrophages (Fig 4G, inset).

Cumulatively, the phenotypical characterization of peripheral tissues of PGT121<sup>+/WT</sup> mice suggests a normal B- and T-cell development, with well-organized secondary lymphoid organs as well as the presence of mature B and T cells. However, we observed a reduction in B-cell progenitors as well as naïve peripheral B cells, pointing toward a possible deletion of PGT121 KI B cells during the early development.

### Sequence analysis of B cells from PGT121 KI mice

Considering that PGT121 KI into our transgenic mice was successfully confirmed via genotyping (Fig 2A) and long-range PCR (Fig 2B), we sought to ascertain whether KI B cells do indeed express PGT121 as part of the BCR. To this end, we isolated and single-cell sorted B cells from bone marrow from heterozygous PGT121<sup>+/WT</sup> mice for IgH sequence analysis. The B-cell progenitors isolated from the bone marrow of these PGT121<sup>+/WT</sup> mice showed a large percentage of B cells with the PGT121 sequence. Interestingly, the presence of PGT121 sequences was restricted to the early immature (B220<sup>+</sup>CD43<sup>+</sup>) B-cell compartment, while no B cells were positive for PGT121 sequences in the late (B220<sup>+</sup>CD43<sup>-</sup>) B-cell compartment (Fig 5A, left; Appendix Table S5).

To assess the frequency of PGT121 germline expression in peripheral mature B cells, we then single-cell sorted (B220<sup>+</sup>IgD<sup>+</sup>) B cells from the blood of two PGT121<sup>+/WT</sup> mice and performed BCR sequencing as above. Our sequencing results revealed that none of the B-cell sequences from the two PGT121<sup>+/WT</sup> mice matched the PGT121 germline sequences. Instead, all the peripheral B cells tested exclusively expressed WT murine IGH sequences (Fig 5A, middle; Appendix Table S6). Comparable results were obtained by sequencing of naïve (B220<sup>+</sup>IgM<sup>+</sup>) B cells from spleen samples (Fig 5A, right; Appendix Table S7). The absence of B cells with PGT121 GL BCRs in the periphery of PGT121<sup>+/WT</sup> mice indicates that the transition of PGT121 B cells from the mouse bone marrow into the blood stream could be impaired, most likely because of autoreactivity and subsequent deletion of PGT121 KI B-cell progenitors.

We analyzed the heavy chain sequences we recovered and compared them with the PGT121 sequence used to generate these KI mice. Sequences from the early immature bone marrow B cells were identical to the original PGT121 sequence used for generating these KI mice, with no mutations or rearrangements (Fig 5A and B). Interestingly, 25% of the sequences recovered from the late B-cell compartment showed a mixed sequence identity, with the antibody V-D regions matching the murine germline repertoire and the J region (partial H-CDR3) matching the PGT121 sequence (Fig 6A). This evidence suggests that the majority of KI B cells positive for PGT121 were eliminated or edited in the bone marrow, and some of these cells might have undergone an event of recombination between the WT murine V-D<sub>1-3</sub> segment, not modified by the

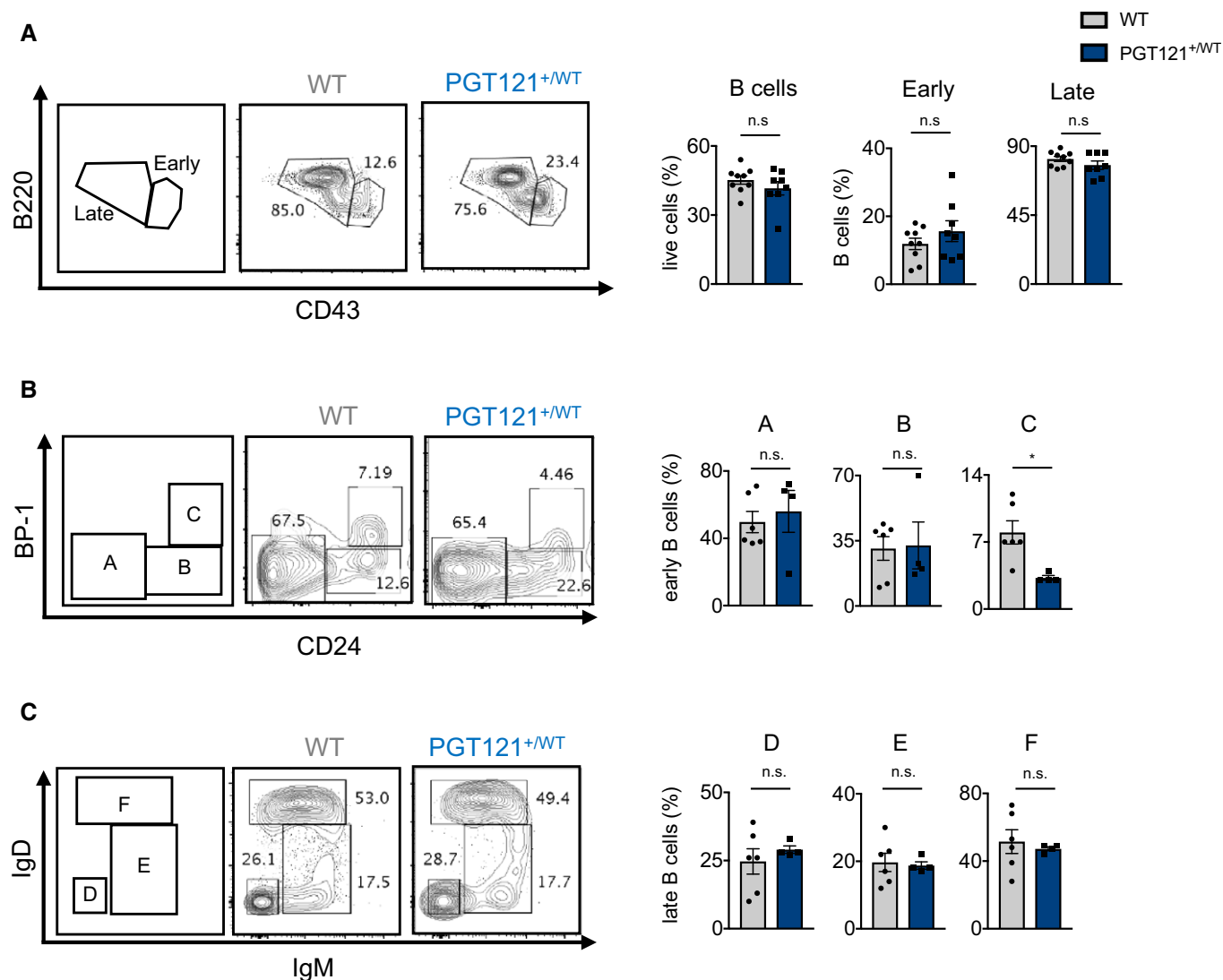


**Figure 3. Characterization of B-lymphocyte development in the bone marrow of PGT121<sup>+/-</sup> mice.**

**A** Bone marrow cells from WT and PGT121<sup>+/-</sup> mice were analyzed by flow cytometry using the gating strategy shown on the left. B-cell progenitors (B220<sup>+</sup>) were divided into immature (CD43<sup>+</sup>) and mature (CD43<sup>-</sup>) cells on the basis of CD43 expression. Data quantified in the panels on the right show the percentage of live cells in the indicated gates (WT: *n* = 9, PGT121<sup>+/-</sup>: *n* = 8, mean ± SEM).

**B** Early (CD43<sup>+</sup>) B-cell progenitors were subdivided according to CD24 and BP-1 expression into Hardy populations A (CD24<sup>-</sup>BP-1<sup>-</sup>), B (CD24<sup>+</sup>BP-1<sup>-</sup>), and C (CD24<sup>+</sup>BP-1<sup>+</sup>). Data quantified in the panels on the right show the percentage of CD43<sup>+</sup> cells in the indicated gates (WT: *n* = 6, PGT121<sup>+/-</sup>: *n* = 4, mean ± SEM).

**C** Late (CD43<sup>-</sup>) B-cell progenitors were subdivided according to IgM and IgD expression into Hardy populations D (IgM<sup>-</sup>IgD<sup>-</sup>), E (IgM<sup>+</sup>IgD<sup>int</sup>), and F (IgM<sup>+</sup>IgD<sup>+</sup>). The data quantified in the panels on the right show the percentage of CD43<sup>-</sup> cells in the indicated gates (WT: *n* = 6, PGT121<sup>+/-</sup>: *n* = 4, mean ± SEM).

Data information: For all flow cytometry experiments, data are from one out of three representative experiments with three or more animals in each group, and each dot represents an individual mouse. Student's *t*-test, ns *P* > 0.05, \**P* < 0.05.

CRISPR/Cas9 machinery, and the inserted PGT121 VDJ sequence, and thereby avoided elimination from the bone marrow (Fig 6B and C).

In one of the 15 PGT121 KI mice, we found the PGT121 heavy chain was inserted in one allelic locus and WT D<sub>4</sub>-J<sub>1-4</sub> segment was deleted in another allele. As such, this mouse will not be able to express the endogenous murine heavy chain variable region. Analysis of this mouse further confirmed the notion that this PGT121 gene was most likely autoreactive since no peripheral

naïve (B220<sup>+</sup>IgD<sup>+</sup>) B cells could be detected by flow cytometry from a homozygous PGT121<sup>+/-</sup> mouse, in which the WT IgH allele had been partially deleted by the CRISPR-mediated double-stranded breaks (D<sub>4</sub> and J<sub>1-4</sub> regions), versus a wild-type mouse (0.07% versus 81.9%, Fig 6D).

Taken together, these data strongly suggest that murine B cells expressing the particular PGT121 germline-reverted heavy chain tested here are defective in clearing immunological checkpoints and are eliminated in the bone marrow.

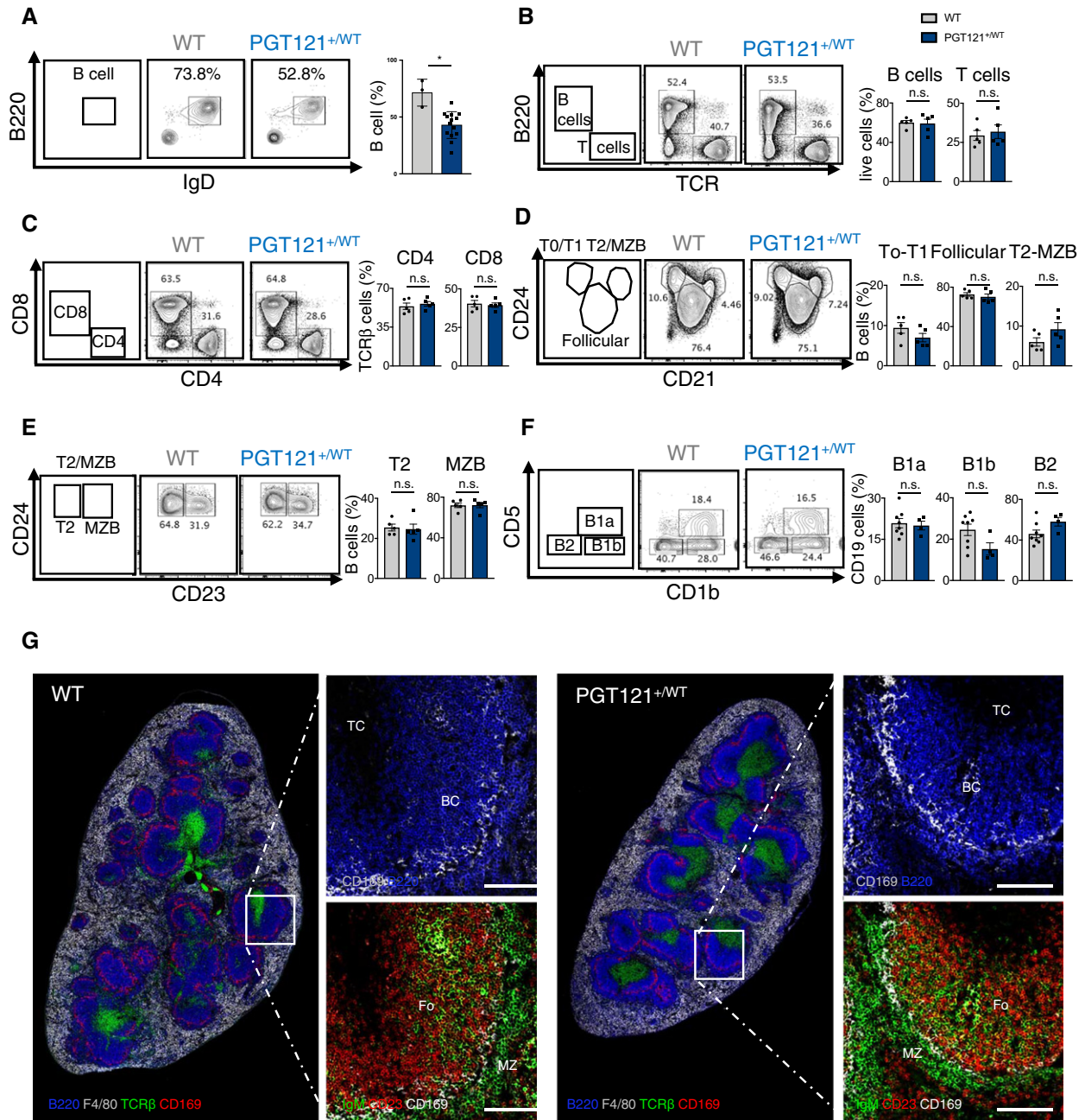


**Figure 4. Characterization of B- and T-lymphocyte development in peripheral blood and spleen of PGT121<sup>+/WT</sup> mice.**

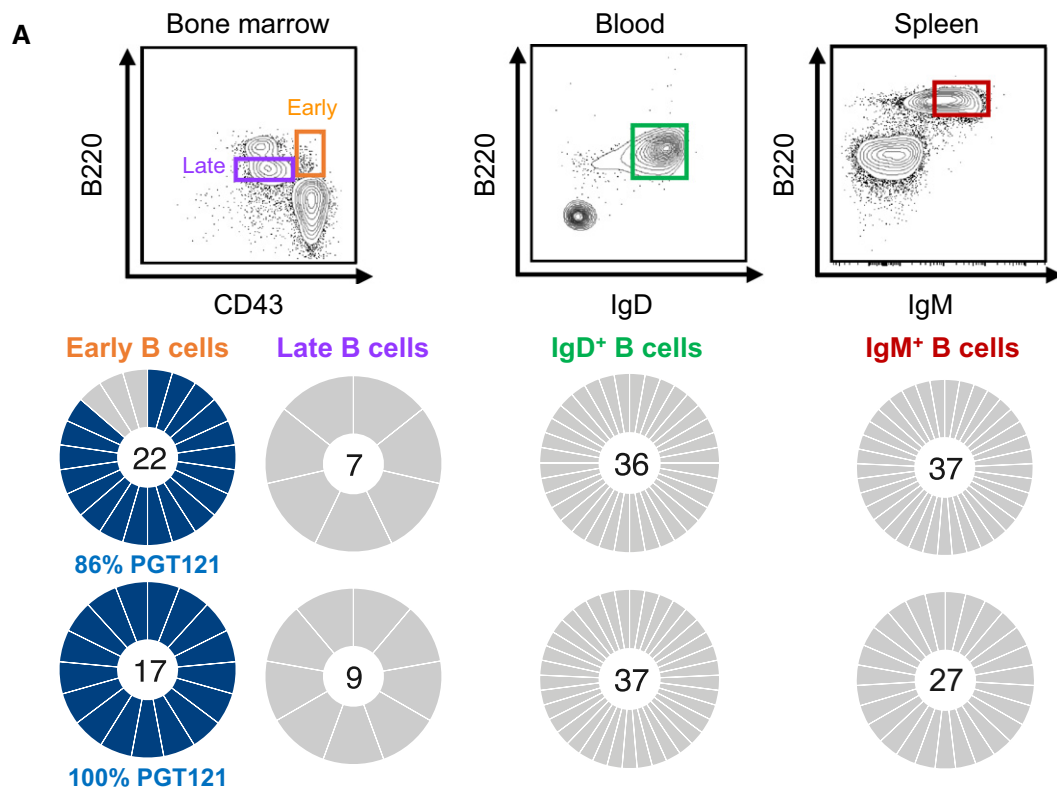
A B cells from blood of WT and PGT121<sup>+/WT</sup> mice were analyzed by flow cytometry. Identification and quantification of B-cell population (B220<sup>+</sup>IgD<sup>+</sup>). Data quantified in the panels on the right show the percentage of live cells in the indicated gates (WT: n = 3, PGT121<sup>+/WT</sup>: n = 14, mean ± SEM).

B–E Splens from WT and PGT121<sup>+/WT</sup> mice were analyzed by flow cytometry. (B, C) Identification and quantification of B cells (B220<sup>+</sup>TCRβ<sup>-</sup>) and T cells (B220<sup>-</sup>TCRβ<sup>+</sup>). T cells were subdivided into CD4 (CD4<sup>+</sup>CD8<sup>-</sup>) and CD8 (CD4<sup>-</sup>CD8<sup>+</sup>) T cells. Quantification—right. (D, E) B cells were divided on the basis of CD21, CD23, and CD24 expression into T0/T1 cells (CD21<sup>hi</sup>CD24<sup>hi</sup>), follicular B cells (CD21<sup>lo</sup>CD24<sup>lo</sup>), T2 cells (CD21<sup>hi</sup>CD24<sup>hi</sup>CD23<sup>-</sup>), marginal zone B (MZB) cells (CD21<sup>hi</sup>CD24<sup>hi</sup>CD23<sup>+</sup>), and quantified (right panels) (n = 5/group, mean ± SEM).

F Peritoneal lavage was performed on WT and PGT121<sup>+/WT</sup> mice, and the exudate was analyzed by flow cytometry. B cells (IgM<sup>+</sup>) were divided into B2 (CD11b<sup>-</sup>CD5<sup>-</sup>), B1b (CD11b<sup>+</sup>CD5<sup>-</sup>), and B1a (CD11b<sup>+</sup>CD5<sup>+</sup>). Data quantified in the panels on the right show the percentage of IgM<sup>+</sup> cells in the indicated gates (WT: n = 8, PGT121<sup>+/WT</sup>: n = 4, mean ± SEM).

G Confocal images spleen cryosections showing the organization of the spleen and the localization of T cells, macrophages, and B cells. Spleen was collected from WT and PGT121<sup>+/WT</sup> mice. Sections were stained with B220 (blue, B cells), CD169 (red, metallophilic macrophages), TCRβ (green, T cells), and F4/80 (white, red pulp macrophages). In the insets, sequential sections were stained for B220 (blue), CD169 (white), IgM (green), and CD23 (red) to identify follicular (Fo, IgM<sup>low</sup>CD23<sup>high</sup>) and marginal zone (MZ, IgM<sup>high</sup>CD23<sup>-</sup>) B cells. TC: T cells, BC: B cells, Fo: follicular B cells, MZ: marginal zone.

Data information: For all flow cytometry experiments (A–F), data are from one out of three representative experiment with three or more animals in each group, and each dot represents an individual mouse. Student's t-test, ns P > 0.05, \*P < 0.05.



**B**

PGT121<sup>+WT</sup>

	FR1	HCDR1	FR2	HCDR2	FR3	HCDR3
	1 10 20 30	30 40 50	40 50 60 70 80	60 70 80 90 100	80 90 100 110 120	100 110 120
PGT121	QVQLQESGPGLVKPSSETLSLTCTVS	GGSISSYY	WSWIRQPPGKGLWIGY	IYYSGST	NYNPSLKSRTVTSVDTSKNQFSLKLSVTAADTAVYYC	ARTLHGITIFGVVAFKEYYYYYYMDVWGK
HC-1	.....	.....	.....	.....	.....	.....
HC-2	.....	.....	.....	.....	.....	.....
HC-3	.....	.....	.....	.....	.....	.....
HC-4	.....	.....	.....	.....	.....	.....
HC-5	.....	.....	.....	.....	.....	.....
HC-6	.....	.....	.....	.....	.....	.....

**Figure 5. Heavy chain sequencing of bone marrow and splenic B cells in the PGT121<sup>+WT</sup> mice.**

A Bone marrow cells from PGT121<sup>+WT</sup> mice were divided into late B cell (B220<sup>int</sup>CD43<sup>low</sup>) and early B cells (B220<sup>int</sup>/hiCD43<sup>+</sup>) on the basis of CD43 expression. B cells from blood of PGT121<sup>+WT</sup> mice were stained for IgD and B220, and spleens from PGT121<sup>+WT</sup> KI mice stained for B220 and IgM. Ig heavy chains from B cells obtained after single-cell sorting were PCR amplified and sequenced. The resulting IGHV libraries from bone marrow, blood, and spleen were compared to our PGT121 sequence to determine sequence identity. The pie charts indicate the frequency of IGHV sequences identical to human PGT121 (blue) and murine IGHV (gray).

B IgH sequences from early immature, bone marrow (B220<sup>+</sup>CD43<sup>+</sup>) B cells. Sequence alignments of 3× representative sequences matching PGT121 from each mouse. Dashes represent identity to the germline reference sequence. FR, framework region; CDR, complementarity-determining region. Amino acid position is indicated with numbers on top of each reference sequence.

**Characterization of B lymphocytes in the BG18 KI mouse**

To further highlight the validity of our novel CRISPR approach, we generated another IgH KI mouse model. To this end, we used the BG18 heavy chain germline-reverted sequence to generate BG18-gH KI mice (hereafter referred to as BG18). BG18 is a recently discovered N332 glycan-dependent bnAb with higher potency but similar breadth as PGT121. BG18-like responses may be easier to elicit than PGT121-like responses, because BG18 does not require any

insertions or deletions (Freund *et al*, 2017). Similar to the characterization of the PGT121 mice, we first determined whether these BG18 KI mice exhibited normal B-cell development in the bone marrow. We observed a similar frequency of early (B220<sup>+</sup>CD43<sup>+</sup>) and late (B220<sup>+</sup>CD43<sup>-</sup>) B cells in the bone marrow of BG18<sup>+WT</sup> mice (Fig 7A). In contrast to the PGT121<sup>+WT</sup> mice, the frequency of B cells in the peripheral blood of BG18<sup>+WT</sup> mice was identical to that of WT mice (Fig 7B, upper). When analyzing the different subpopulations of peripheral B cells, the frequencies of IgD<sup>+</sup> and



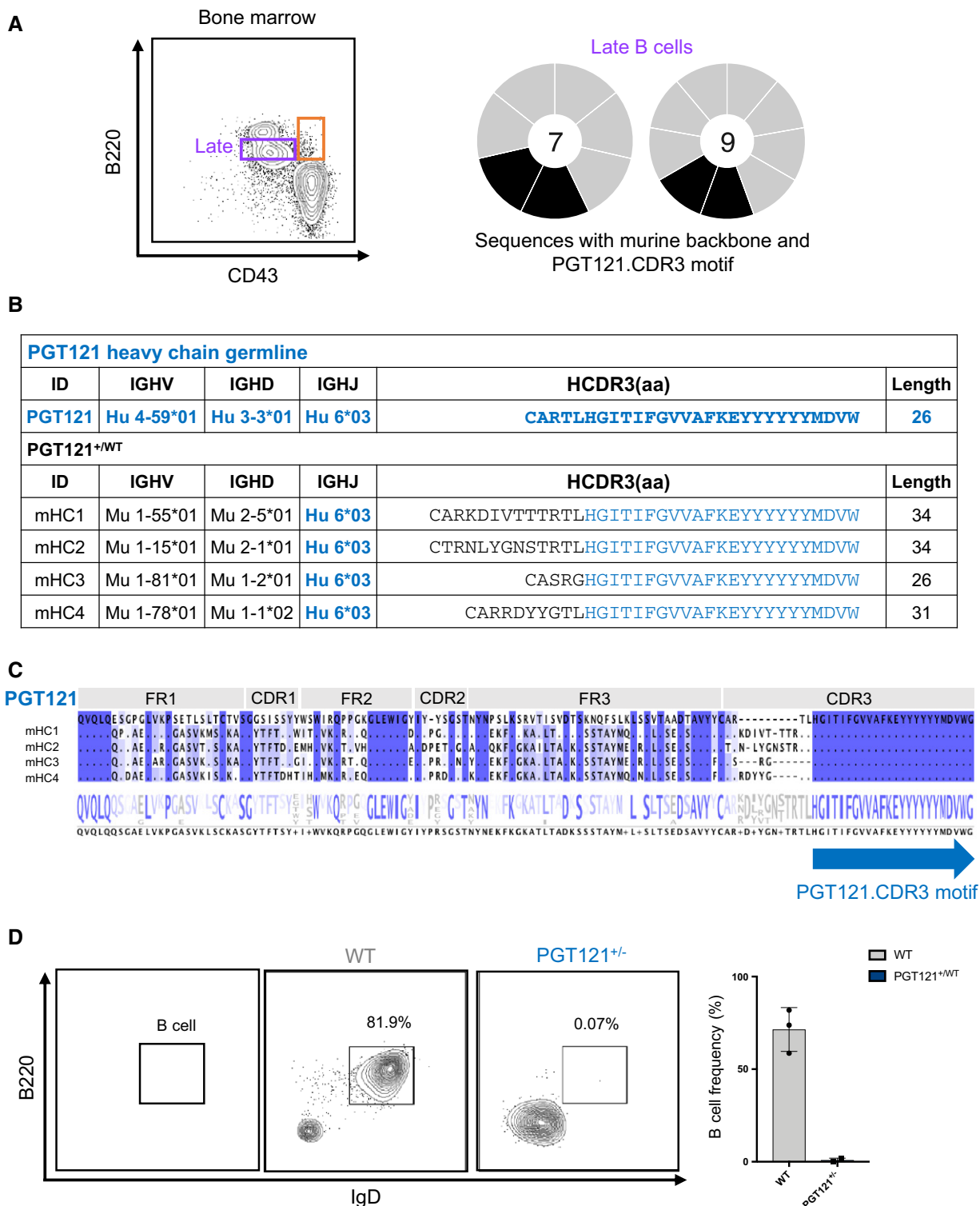


**Figure 6. Sequence analysis of PGT121 sequences recovered from bone marrow B-cell progenitors.**

A, B Bone marrow B cells from two PGT121<sup>+WT</sup> mice were stained for B220 and CD43. Late B cells (B220<sup>int</sup>CD43<sup>low</sup>) were single-cell sorted for antibody heavy chain and subjected to PCR amplification and sequencing. 2/7 (or 28.5%) and 2/9 (22.2%) of the murine IGHV sequences isolated from late B cells exhibited CDR3 motif of PGT121, depicted in blue lettering.

C The four murine IGHV sequences were aligned to the germline-reverted PGT121 heavy chain (blue). The CDR3 motif HGITIFGVVAFKEYYYYYYMDVW of PGT121 was found in all four murine IGHV sequences (indicated by blue arrow). CDR: complementarity-determining region, FR: framework region.

D B cells from peripheral blood of WT or PGT121<sup>+/-</sup> mice were analyzed by flow cytometry. Identification and quantification of B-cell population (B220<sup>+</sup>IgD<sup>+</sup>) (WT: *n* = 3, PGT121<sup>+/-</sup>: *n* = 2, mean ± SEM)

IgM<sup>+</sup> B cells were comparable in BG18<sup>+/WT</sup> and WT mice (Fig 7B, lower). Moreover, we observed no impact on the percentage of T cells between the BG18<sup>+/WT</sup> versus WT mice (Fig 7B, upper). In one of the BG18 KI mice, called BG18<sup>+/-</sup>, the BG18 heavy chain was inserted in one of the murine IgH D<sub>4</sub>-J<sub>1.4</sub> allelic loci. In addition, in this mouse, the WT D<sub>4</sub>-J<sub>1.4</sub> segment was deleted in the other allele of the same locus. In the BG18<sup>+/-</sup> mice, the frequency of B cells in the periphery was reduced when compared to the WT animals (Fig 7C); however, since B cells bearing the BG18 heavy chain can still be found in the periphery, these results indicate that immunological checkpoints are not affected in this mouse line. In these mice, the gross pathological analysis of spleen from the BG18<sup>+/WT</sup> and BG18<sup>+/-</sup> mice reflected normal development. Upon histological examination, we identified normal structures of the white and red pulp by confocal microscopy (Fig 7D). Both BG18<sup>+/WT</sup> and BG18<sup>+/-</sup> mice presented a normal organization of T cells, B cells, and metallophilic macrophages in the white pulp and F4/80<sup>+</sup> macrophages in the red pulp. No alterations were observed in the composition of the B-cell populations, and we identified both follicular (CD23<sup>high</sup>IgM<sup>low</sup>) and marginal zone B cells (CD23<sup>-</sup>IgM<sup>+</sup>) in a correct proportion (Fig 7D, inset).

#### BG18 KI mice express BG18 germline heavy chain at high frequency

Upon observing no adverse impact on B-cell development in the BG18 KI mice, we isolated and single-cell sorted splenic B cells of these mice and proceeded to determine the frequency of BG18 germline sequences via BCR sequencing. We obtained B220<sup>+</sup>IgM<sup>+</sup> B splenocytes from two BG18<sup>+/WT</sup> mice and one BG18<sup>+/-</sup> mouse. In the BG18<sup>+/WT</sup> mice, 30 to 32% of the analyzed sequences were identical to the BG18 germline sequence, while the majority of sequences (90%) corresponding to B cells isolated from the BG18<sup>+/-</sup> mouse were identical to the BG18 germline sequence (Fig 8A, right). When comparing the BG18 sequences obtained from splenic B cells to the original germline sequence used to generate these mice, we observed the following: (i) BG18GL sequences from the majority (90%) of single B cells sequenced showed no mutations (Fig 8B; Appendix Table S8); and (ii) sequences from 10% of naïve B cells from the BG18 KI mouse showed a mixed identity, with mouse V regions recombined with the human D-J region (BG18 CDR3) due to mosaicism or an early recombination event (Fig EV5). Taken collectively, our results suggest that the BG18 KI mouse represents a valuable model, which can be used to test BG18-specific immunogens.

## Discussion

Genetically engineered mice have been invaluable models in the study of humoral responses. The introduction of pre-defined monoclonal heavy or light chain antibody sequences into the genome of recipient mice made it possible to dissect fundamental biological processes, from the early selection of the BCR in bone marrow B-cell progenitors to how these antibodies evolve in response to antigenic challenge (Weaver *et al*, 1985; Nussenzweig *et al*, 1987; Manz *et al*, 1988; Goodnow *et al*, 1989; Bloom *et al*, 1993; Benschop *et al*, 2001; Jardine *et al*, 2015). In this study, we demonstrate the use of the CRISPR/Cas9 technology for the one-step generation of mice harboring a 1.9 kb pre-arranged human heavy chain in the murine IgH locus in a short time with an average efficiency of 40%. These results constitute a major advance that will allow the rapid and reproducible generation of such mouse models for evaluating the efficacy of novel immunogens and sequential immunization regimens, including but not limited to regimens intending to elicit protective responses starting from activation of specific human naïve B-cell precursors. Ultimately, we expect these mouse models will accelerate the pace of vaccine development against particularly recalcitrant agents of infectious disease.

In the past, genetic KI mice have not only been crucial in elucidating B-cell functions but also as models to interrogate efficacy of immunogens to potentially function as vaccines (Dosenovic *et al*, 2015; Jardine *et al*, 2015; Escolano *et al*, 2016). The generation of these traditional KI mice was reliant on targeting genetic loci in ES cells via homologous recombination to generate mice with desired mutations (Verkoczy *et al*, 2017). This method, however, is laborious and time-consuming as it may take 2 years or more to produce homozygous animals from transmitted germline and heterozygous mice (Capecchi, 2005). This is because gene targeting in ES cells is very inefficient and can take up to 2 years. Also, targeted ES cells need to be implanted into blastocysts, which lead to high chimerism in founder mice. Often germline transmission is not achieved. More recently, a methodology termed RDBC (Rag2-deficient blastocyst complementation) was developed to first introduce human BCRs into ES cells and then inject into Rag2<sup>-/-</sup> blastocyst to generate chimeric mice (Chen *et al*, 1993; Tian *et al*, 2016). Although the F0 mice are chimeric, all B- and T-cell receptors in these mice are derived from these ES cells, and as a result, these mice can be readily used in immunocharacterization studies. Although the RDBC method obviates the time spent in breeding mice for the germline

#### Figure 7. Characterization of B-lymphocyte development in BG18 KI mice.

- A Bone marrow cells from WT and BG18<sup>+/WT</sup> mice were analyzed by flow cytometry using the gating strategy shown on the left. B-cell progenitors (B220<sup>+</sup>) were divided into immature (CD43<sup>+</sup>) and mature (CD43<sup>-</sup>) cells on the basis of CD43 expression. Data quantified in the panels on the right show the percentage of live cells in the indicated gates ( $n = 3/\text{group}$ , mean  $\pm$  SEM)
- B Blood from WT and BG18<sup>+/WT</sup> mice was analyzed by flow cytometry. Identification and quantification of B cells (B220<sup>+</sup>TCR $\beta$ <sup>-</sup>) and T cells (B220<sup>-</sup>TCR $\beta$ <sup>+</sup>). B cells were subdivided into mature (IgD<sup>+</sup>) and T1 (IgD<sup>-</sup>IgM<sup>+</sup>) B cells. Quantification—right (WT:  $n = 4$ , BG18<sup>+/WT</sup>:  $n = 9$ , mean  $\pm$  SEM)
- C B cells from blood of WT or BG18<sup>+/-</sup> mice were analyzed by flow cytometry. Identification and quantification of B cells (B220<sup>+</sup>TCR $\beta$ <sup>-</sup>) and T cells (B220<sup>-</sup>TCR $\beta$ <sup>+</sup>) (WT:  $n = 6$ , BG18<sup>+/WT</sup>:  $n = 3$ , mean  $\pm$  SEM).
- D Confocal images spleen cryosections showing the organization of the spleen and the localization of T cells, macrophages, and B cells. Spleen was collected from BG18<sup>+/WT</sup> and BG18<sup>+/-</sup> mice. Sections were stained with B220 (blue, B cells), CD169 (red, metallophilic macrophages), TCR $\beta$  (green, T cells), and F4/80 (white, red pulp macrophages). In the insets, sequential sections were stained for B220 (blue), CD169 (white), IgM (green), and CD23 (red) to identify follicular (Fo, IgM<sup>low</sup>CD23<sup>high</sup>) and marginal zone (MZ, IgM<sup>high</sup>CD23<sup>-</sup>) B cells. TC: T cells, BC: B cells, Fo: follicular B cells, MZ: marginal zone.

Data information: For all flow cytometry experiments (A–C), data are from one out of three representative experiments with three or more animals in each group, and each dot represents an individual mouse. Student's *t*-test, ns  $P > 0.05$ , \*\* $P < 0.01$ .

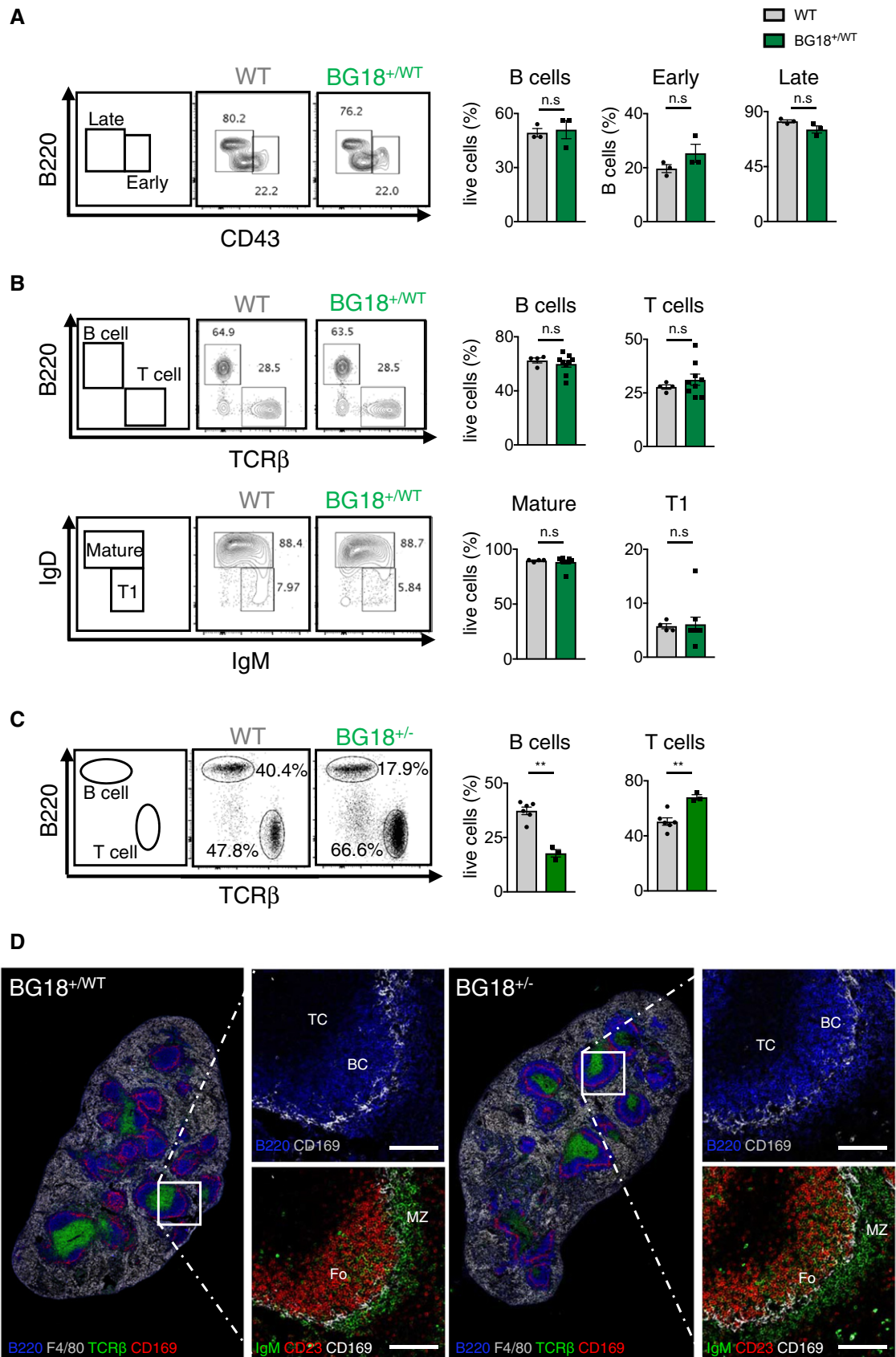
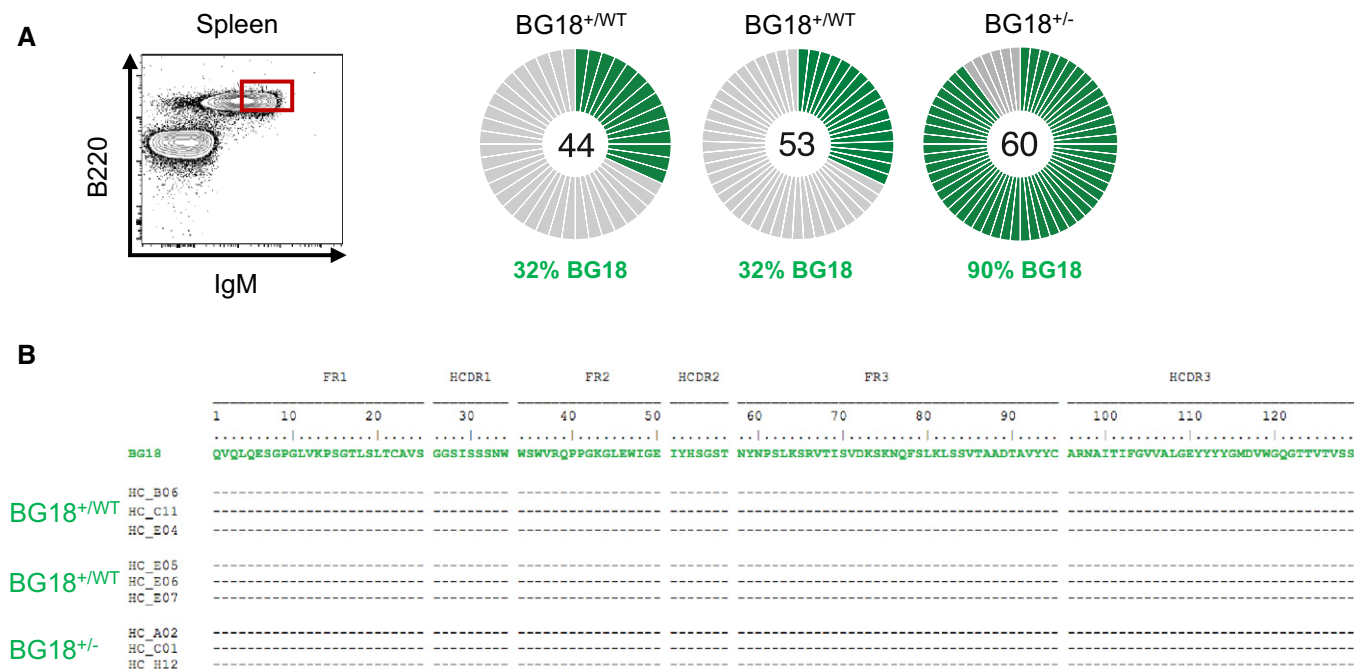


Figure 7.



**Figure 8. Heavy chain sequencing of splenic B cells in the BG18 KI mice.**

- A** B cells from spleens from BG18<sup>+/WT</sup> or BG18<sup>+/-</sup> KI mice stained for B220 and IgM. Ig heavy chains from B cells obtained after single-cell sorting were PCR amplified and sequenced. The resulting IGHV libraries from spleen were compared to our BG18 sequence to determine sequence identity. The pie charts indicate the frequency of IGHV sequences identical to human BG18 (green) and murine IGHV (gray).
- B** IgH sequences from splenic (B220<sup>+</sup>IgM<sup>+</sup>) B cells. Sequence alignments of 3× representative sequences matching BG18 from each mouse. Dashes represent identity to the germline reference sequence. FR, framework region; CDR, complementarity-determining region. Amino acid position is indicated with numbers on top of each reference sequence.

transmission of transgenic BCRs, the generation of bona fide homozygous KI mice still requires several months to select (Oji *et al*, 2016). In contrast, the novelty of our one-step CRISPR injection approach lies in the generation of F0 founder mice harboring the germline transmission of the transgenic BCR (Figs 2C and EV4).

Our method represents a significant improvement over the already revolutionary CRISPR gene modification methods, because until now the insertion of relatively large DNA fragments via CRISPR/Cas9 was considered a challenge. The bottleneck with the earlier iterations of the CRISPR/Cas9 methodology lays in the limitation on the length of DNA donors bearing gene modifications. The allowable length of DNA donors for small gene modifications is < 200 bp, with these donors being synthesized as a single-stranded DNA oligodeoxynucleotides (ssODN) (Jacobi *et al*, 2017). For large DNA insertions requiring > 200 bp of DNA donor, generally dsDNA plasmid templates with at least 800-bp homology arms are constructed (Jacobi *et al*, 2017). However, such plasmid templates reduce the efficiency of CRISPR targeting in loci other than *ROSA26*, where the integration of an 8- to 11-kb DNA fragment by CRISPR injection with a 10–20% homologous recombination rate has been reported (Awatramani *et al*, 2001; Chu *et al*, 2016). The *ROSA26* locus is a well-characterized region in chromosome 6 that offers an open chromatin configuration. Therefore, it can be easily modified by homologous recombination to express transgenes ubiquitously in embryonic and adult mice (Soriano, 1999). Recently, the Easi-CRISPR (Efficient additions with ssDNA inserts-CRISPR) method,

based on the use of 0.8- to 1.6-kb-long single-strand DNA as a repair template, has been shown to be highly effective in generating KI mice expressing knock-in alleles for over a dozen loci (Quadros *et al*, 2017). In contrast to this approach, our methodology relies on a double-stranded repair template with > 2-kb homology arms, which is over the limit of commercial ssDNA. In the future, it would be interesting to determine whether this method will result in the improved frequency of immunoglobulin KI animals.

Upon generating the PGT121 germline heavy chain KI mice, we examined the impact of its insertion on B-lymphocyte development. Although the composition of peripheral B- and T-cell populations appeared to be normal in these mice, we noticed a lack of PGT121-bearing B cells, as all the antibodies generated by these mice contained murine IgH sequences. For this reason, we investigated the B-cell progenitors in the bone marrow and secondary lymphoid organs, and we observed a reduction in early pre-B cells (Hardy fraction C), indicating a possible negative effect of PGT121 germline heavy chain expression in this stage of B-cell development (Hardy *et al*, 1991). Indeed, when we analyzed the bone marrow B cells for the presence of PGT121 sequences, KI cells were present only in the immature (B220<sup>+</sup>CD43<sup>+</sup>BP-1<sup>+</sup>) B-cell population of the bone marrow. The fate of early pre-B cells is determined by the correct expression of a functional pre-BCR, in a process known as positive selection. Cells that fail the V(D)J recombination or express autoreactive antibodies are destined to be eliminated or edited (Pelanda *et al*, 1997; Pewzner-Jung *et al*, 1998). Although the previously

tested PGT121 broadly neutralizing antibody exhibits no polyreactivity and autoreactivity *in vitro* and the previously generated PGT121<sub>CDR3rev4</sub> mouse model also does not exhibit defects in B-cell development (Liu *et al*, 2015), our results indicate that B cells expressing the PGT121-gH, described here, were eliminated (Figs 5 and EV1). This phenomenon of BCR exclusion has also been described in the case of other human immunoglobulins (Verkoczy *et al*, 2010, 2011; Doyle-Cooper *et al*, 2013).

Our CRISPR/Cas9 approach was used to generate another germ-line-reverted bnAb knock-in: BG18. BG18 is a recently discovered bnAb directed against the glycan-V3 epitope of HIV-1 Env (Freund *et al*, 2017). Recently, the crystal structure of BG18 complexed with native HIV Env trimers was solved, and the Env epitope that facilitates antibody recognition and virus neutralization was identified (Barnes *et al*, 2018). However, currently it is unclear how B-cell precursors corresponding to BG18-GL respond to specific immunogens. Of specific interest is whether the BG18-GL IgH accumulates adequate somatic hypermutations and matures into functional memory B cells capable of rapid and durable antibody response. Our BG18-GL IgH KI mouse will allow us to evaluate the efficacy of novel HIV-1 immunogens to elicit protective immunoresponses. Indeed, in this mouse line, functional B cells bearing BG18-GL sequences are normally expressed in spleen and periphery.

Although the first mouse line, PGT121 KI that we generated, is unsuitable for immunogen testing, the BG18 KI mouse does not suffer from this drawback. Therefore, we believe that we are in a position to generate several other immunoglobulin mouse variants and rapidly assess which animals could be advanced for immunogen testing. Furthermore, although heavy chains represent main components of antibodies, light chains may also be required for full specificity. Given the high frequency of HDR directed by two sgRNAs in our current approach, we would like to extend our method to generate light chain KI mice. Future work could also involve the generation of mice bearing heavy and light chains with one single injection with two donor plasmids.

## Materials and Methods

### sgRNA selection, screening, preparation, and validation

sgRNAs were identified using the <http://crispr.mit.edu/> (Appendix Table S1). *In vitro* sgRNA syntheses were performed using the EnGen<sup>®</sup> sgRNA Synthesis Kit, *S. pyogenes* (NEB) following the manufacturer's instructions. Transcribed sgRNAs were purified by using MEGAclean<sup>™</sup> Transcription Clean-Up Kit (Ambion<sup>®</sup>) following the manufacturer's instructions. PCR amplification of genomic DNA fragments from C57Bl/6 control mice (target and off-target) was performed using gene-specific primers (Appendix Table S3) under the following conditions: 98°C for 2 min; 40× (98°C for 20 s, 55°C for 30 s, and 72°C for 1 min); 72°C for 5 min; hold at 4°C; and subsequently sequenced. sgRNA validation was performed by using *in vitro* digestion with Cas9 nuclease, *S. pyogenes* assay (NEB) following the manufacturer's instructions. Briefly, each reaction containing 20 μl of nuclease-free H<sub>2</sub>O, 3 μl of 10× Cas9 buffer, 3 μl sgRNA (300 nM), and 1 μl Cas9 (1 μM) was incubated for 10 min at room temperature (RT). Subsequently, 3 μl of DNA (30 nM) was added to each reaction and incubated at 37°C for 1 h.

Samples were separated through a 1% agarose gel or 5% TBE gel in TBE buffer (5% Mini-PROTEAN<sup>®</sup> TBE Gel, #4565016, Bio-Rad) and stained with SYBR Safe. Images were captured using a Gel Doc<sup>™</sup> EZ Gel Documentation System (Bio-Rad).

### Generation of targeting vectors

The VRC01 gH vector backbone (Jardine *et al*, 2015) was modified by replacing the neomycin cassette with rearranged VDJ sequences for human bnAb germline precursors PGT121 and BG18 downstream of the promoter region and by elongation of the 5' and 3' homology regions utilizing the Gibson assembly method (NEB). The targeting vector DNA was confirmed by Sanger sequencing (Eton Bioscience Inc).

### Generation of KI mice

sgRNAs, donor DNA, and Cas9 protein (PNA BIO INC) were provided to the Genome Modification Facility at Harvard University for the generation KI mice by CRISPR/Cas9 method (Ran *et al*, 2013; Yang *et al*, 2014). Briefly, we prepared injection mix of Cas9 protein (50 ng/μl), each sgRNA (25 ng/μl), and circular DNA donor (200 ng/μl) in injection buffer and performed microinjecting 200 fertilized oocytes. After culturing the injected zygotes, we transfer zygotes to pseudopregnant foster mothers.

### Mice breeding for maintenance and experiments

Initial mice breeding of F1 generation was performed at the animal facility of the Gene Modification Facility (Harvard University). Breeding for colony expansion and experimental procedures was performed and the Ragon Institute. All experiments were approved by the Institutional Animal Care and Use Committee (IACUC) of Harvard University and the Massachusetts General Hospital and conducted in accordance with the regulations of the American Association for the Accreditation of Laboratory Animal Care (AAALAC).

### Genotyping and long-range PCR

Ear or tail snips were used for genotyping. All of the mice were genotyped by TaqMan assay for a fee for service agreement (TransnetYX). TaqMan probes for the genotyping assay were developed by TransnetYX. Genomic DNA was purified from tail DNA using the Viagen DirectPCR Lysis Reagent (Viagen Biotech Inc., CA, USA) supplemented with proteinase K solution (0.1 mg/ml final, Roche) in a total volume of 250 μl. Reactions were incubated at 55°C overnight and at 85°C for an additional 40 min. Debris was pelleted by centrifugation at 12,000 × *g* for 2 min and the supernatant collected. Long-range PCR amplification of genomic DNA fragments from C57Bl/6 control mice or KI mice was performed using specific primers (Appendix Table S3) under the following conditions: 98°C for 2 min; 40× (98°C for 20 s, 61.2°C for 30 s, and 72°C for 2 min); 72°C for 5 min; and hold at 4°C.

### Flow cytometry and single-cell sorting

Single-cell suspensions were prepared from spleen, lymph nodes, bone marrow, peritoneal lavage, or peripheral blood samples. Red

blood cells were removed by ACK lysis (Life Technologies). Cells were prepared in FACS buffer (2% FCS/PBS) and enumerated, and Fc receptors were blocked using anti CD16/32 antibodies (BD Pharmingen). Subsequently, cells were stained with the appropriate combination of the following antibodies (Invitrogen, BioLegend, BD Pharmingen) for 30 min at 4°C and washed twice before analysis: B220 (RA3-6B2), TCR $\beta$  (H57-597), CD21 (CR2/CR1), CD4 (GK1.5, RM4-5), CD8 (53-6.7), CD23 (B3B4), CD24 (30-F1), CD43 (S11), CD5 (53-7.3), IgM (RMM1), IgD (11-26c.2a), CD40 (3/23), CD249 (BP-1) (6C3), (BioLegend). Data were acquired on a LSR Fortessa, LSRII (BD Bioscience), or SH800 (Sony) and analyzed with FlowJo 10 (Treestar). Staining of the cells with Live-Dead kits (Thermo Scientific) was used to identify dead cells for exclusion from the analysis.

### BCR sequencing

Individual PGT121 and WT B cells were single-cell sorted on Aria Fusion (BD Bioscience) or SH800 (Sony) into 96-well PCR plates directly into lysis buffer [0.1 M Trizma HCl pH 8 (Sigma), 500 U/ml RNase inhibitor (NEB)] and frozen immediately on dry ice. Plates were stored at 80°C until further processing. Naïve B cells were defined as scatter, singlet, live, B220<sup>+</sup>, IgM<sup>+</sup>.

First-strand cDNA synthesis was carried out using SuperScript III Reverse Transcriptase (Invitrogen) according to manufacturer's instructions. Nested PCR reactions were performed using Hot-StarTaq polymerase (Qiagen) and IgM-specific primer pools (Appendix Table S4), also described previously (von Boehmer *et al*, 2016). Each round of PCR was performed using the indicated primers (30 nM) and 2.5  $\mu$ l of cDNA template (first or second PCR product) under the following conditions: 45 $\times$  [94°C for 30 s, 46°C/50°C (first and second PCR product, respectively) for 30 s, 72°C for 55 s/40 s (first and second PCR product, respectively)]. PCR products were separated through a 2% e-GEL (Thermo Scientific) to confirm amplification. Samples with fragments of the correct size were purified and sequenced by Sanger method (Genewiz). Heavy chain products were sequenced using the IgM-specific reverse primer from the second PCR reaction. Sequences were quality-checked, and Ig gene assignments were carried out via IMGT/V-QUEST.

### Immunohistochemistry and microscopy

For surface staining, frozen spleen sections (10  $\mu$ m) were dried, fixed in 4% PFA for 10 min, blocked with PBS 5% normal goat serum (NGS), and then incubated with a combination of the following anti-mouse antibodies in 1% BSA for 1 h: B220 Pacific Blue (RA3-6 B2), TCR $\beta$  AF488 (H57-597), CD23 APC (B3B4), IgM AF488 (RMM-1), F4/80 APC (BM8), CD169 (Siglec-1) AF555 (MOMA-1), (BioLegend). Sections were mounted with ProLong Gold antifade reagent (Thermo Scientific). Images were acquired on a LSM 780 (Zeiss) inverted confocal microscope using a Plan-Apochromat 20 $\times$  objective.

### Experimental data and statistical analysis

Statistical parameters including the exact value of  $n$  with the description of what  $n$  represents, the mean, the SEM, and the  $P$ -value are reported in the Figures and the Figure Legends. Statistical

analyses were performed using Prism (GraphPad Software) and compared with Student's  $t$ -test,  $P$ -values < 0.05 were considered significant. In figures, asterisks stand for \* $P$  < 0.05; \*\* $P$  < 0.01.

**Expanded View** for this article is available online.

### Acknowledgements

This work was supported by the Ragon Institute of MGH, MIT, and Harvard (F.D.B.); NIAID UM1AI100663 (CHAVI-ID) (W.R.S., F.D.B.); by the International AIDS Vaccine Initiative Neutralizing Antibody Consortium and Center (W.R.S.); and CAVD funding for the IAVI NAC Center (W.R.S.). We thank David Nemazee, The Scripps Research Institute, for the kind gift of the VRC01 plasmid.

### Author contributions

FDB and WRS provided the project outline and were instrumental in the design of experiments. SP and Y-CL helped design and perform experiments, analyzed the data, and together with UN and FDB composed the manuscript. EM performed immunohistochemistry staining and microscopy. SK together with SP isolated and single-cell sorted B cells for sequencing and analyzed the data with support from JMS. Together with UN and input from SKD, Y-CL designed and implemented the CRISPR approach. Microinjections were performed by LW and KHK coordinated mouse sample collection and work. Y-CL carried out the experimental mouse protocols with assistance from SP, SK, EM, and JA. All the authors provided critical feedback on the manuscript prior to publication and have agreed to the final content.

### Conflict of interest

The authors declare that they have no conflict of interest.

### References

- Aman MJ, Ravichandran KS (2000) A requirement for lipid rafts in B cell receptor induced Ca(2+) flux. *Curr Biol* 10: 393–396
- Awatramani R, Soriano P, Mai JJ, Dymecki S (2001) An Flp indicator mouse expressing alkaline phosphatase from the ROSA26 locus. *Nat Genet* 29: 257–259
- Barnes CO, Gristick HB, Freund NT, Escolano A, Lyubimov AY, Hartwegner H, West AP, Cohen AE, Nussenzweig MC, Bjorkman PJ (2018) Structural characterization of a highly-potent V3-glycan broadly neutralizing antibody bound to natively-glycosylated HIV-1 envelope. *Nat Commun* 9: 1251
- Batista FD, Neuberger MS (2000) B cells extract and present immobilized antigen: implications for affinity discrimination. *EMBO J* 19: 513–520
- Benschop RJ, Aviszus K, Zhang X, Manser T, Cambier JC, Wysocki LJ (2001) Activation and anergy in bone marrow B cells of a novel immunoglobulin transgenic mouse that is both hapten specific and autoreactive. *Immunity* 14: 33–43
- Bloom DD, Davignon JL, Cohen PL, Eisenberg RA, Clarke SH (1993) Overlap of the anti-Sm and anti-DNA responses of MRL/Mp-lpr/lpr mice. *J Immunol* 150: 1579–1590
- von Boehmer L, Liu C, Ackerman S, Gitlin AD, Wang Q, Gazumyan A, Nussenzweig MC (2016) Sequencing and cloning of antigen-specific antibodies from mouse memory B cells. *Nat Protoc* 11: 1908–1923
- Briney B, Sok D, Jardine JG, Kulp DW, Skog P, Menis S, Jacak R, Kalyuzhnyi O, de VN, Sesterhenn F, Le KM, Ramos A, Jones M, Saye-Francisco KL, Blane TR, Spencer S, Georgeson E, Hu X, Ozorowski G, Adachi Y *et al* (2016) Tailored immunogens direct affinity maturation toward HIV neutralizing antibodies. *Cell* 166: 1459–1470.e11

- Capecchi MR (2005) Gene targeting in mice: functional analysis of the mammalian genome for the twenty-first century. *Nat Rev Genet* 6: 507–512
- Chen J, Lansford R, Stewart V, Young F, Alt FW (1993) RAG-2-deficient blastocyst complementation: an assay of gene function in lymphocyte development. *Proc Natl Acad Sci USA* 90: 4528–4532
- Chu VT, Weber T, Graf R, Sommermann T, Petsch K, Sack U, Volchkov P, Rajewsky K, Kühn R (2016) Efficient generation of Rosa26 knock-in mice using CRISPR/Cas9 in C57BL/6 zygotes. *BMC Biotechnol* 16: 4
- Dal Porto JM, Haberman AM, Kelsoe G, Shlomchik MJ (2002) Very low affinity B cells form germinal centers, become memory B cells, and participate in secondary immune responses when higher affinity competition is reduced. *J Exp Med* 195: 1215–1221
- Dosenovic P, von Boehmer L, Escolano A, Jardine J, Freund NT, Gitlin AD, McGuire AT, Kulp DW, Oliveira T, Scharf L, Pietzsch J, Gray MD, Cupo A, van Gils MJ, Yao K-H, Liu C, Gazumyan A, Seaman MS, Björkman PJ, Sanders RW et al (2015) Immunization for HIV-1 broadly neutralizing antibodies in human Ig knockin mice. *Cell* 161: 1505–1515
- Dougan SK, Ogata S, Hu C-CA, Grotenbreg GM, Guillen E, Jaenisch R, Ploegh HL (2012) IgG1 + ovalbumin-specific B-cell transnuclear mice show class switch recombination in rare allelically included B cells. *Proc Natl Acad Sci USA* 109: 13739–13744
- Doyle-Cooper C, Hudson KE, Cooper AB, Ota T, Skog P, Dawson PE, Zwick MB, Schief WR, Burton DR, Nemazee D (2013) Immune tolerance negatively regulates B cells in knock-in mice expressing broadly neutralizing HIV antibody 4E10. *J Immunol* 191: 3186–3191
- Escolano A, Steichen JM, Dosenovic P, Kulp DW, Golijanin J, Sok D, Freund NT, Gitlin AD, Oliveira T, Araki T, Lowe S, Chen ST, Heinemann J, Yao K-H, Georgeson E, Saye-Francisco KL, Gazumyan A, Adachi Y, Kubitz M, Burton DR et al (2016) Sequential immunization elicits broadly neutralizing anti-HIV-1 antibodies in Ig knockin mice. *Cell* 166: 1445–1458.e12
- Freund NT, Wang H, Scharf L, Nogueira L, Horwitz JA, Bar-On Y, Golijanin J, Sievers SA, Sok D, Cai H, Cesar Lorenzi JC, Halper-Stromberg A, Toth I, Piechocka-Trocha A, Gristick HB, van Gils MJ, Sanders RW, Wang L-X, Seaman MS, Burton DR et al (2017) Coexistence of potent HIV-1 broadly neutralizing antibodies and antibody-sensitive viruses in a viremic controller. *Sci Transl Med* 9: eaal2144
- Gatto D, Paus D, Basten A, Mackay CR, Brink R (2009) Guidance of B cells by the orphan G protein-coupled receptor EBI2 shapes humoral immune responses. *Immunity* 31: 259–269
- Goodnow CC, Crosbie J, Adelstein S, Lavoie TB, Smith-Gill SJ, Brink RA, Pritchard-Briscoe H, Wotherspoon JS, Loblay RH, Raphael K (1988) Altered immunoglobulin expression and functional silencing of self-reactive B lymphocytes in transgenic mice. *Nature* 334: 676–682
- Goodnow CC, Crosbie J, Jorgensen H, Brink RA, Basten A (1989) Induction of self-tolerance in mature peripheral B lymphocytes. *Nature* 342: 385–391
- Hao S, August A (2005) Actin depolymerization transduces the strength of B-cell receptor stimulation. *Mol Biol Cell* 16: 2275–2284
- Hardy RR, Carmack CE, Shinton SA, Kemp JD, Hayakawa K (1991) Resolution and characterization of pro-B and pre-pro-B cell stages in normal mouse bone marrow. *J Exp Med* 173: 1213–1225
- Jacobi AM, Rettig GR, Turk R, Collingwood MA, Zeiner SA, Quadros RM, Harms DW, Bonthuis PJ, Gregg C, Ohtsuka M, Gurumurthy CB, Behlke MA (2017) Simplified CRISPR tools for efficient genome editing and streamlined protocols for their delivery into mammalian cells and mouse zygotes. *Methods* 121–122: 16–28
- Jardine JG, Ota T, Sok D, Pauthner M, Kulp DW, Kalyuzhnyi O, Skog PD, Thinnis TC, Bhullar D, Briney B, Menis S, Jones M, Kubitz M, Spencer S, Adachi Y, Burton DR, Schief WR, Nemazee D (2015) HIV-1 vaccines. Priming a broadly neutralizing antibody response to HIV-1 using a germline-targeting immunogen. *Science* 349: 156–161
- Joyce MG, Wheatley AK, Thomas PV, Chuang G-Y, Soto C, Bailer RT, Druz A, Georgiev IS, Gillespie RA, Kanekiyo M, Kong W-P, Leung K, Narpala SN, Prabhakaran MS, Yang ES, Zhang B, Zhang Y, Asokan M, Boyington JC, Bylund T et al (2016) Vaccine-induced antibodies that neutralize group 1 and group 2 influenza A viruses. *Cell* 166: 609–623
- Julien JP, Cupo A, Sok D, Stanfield RL, Lyumkis D, Deller MC, Klasse PJ, Burton DR, Sanders RW, Moore JP, Ward AB, Wilson IA (2013) Crystal structure of a soluble cleaved HIV-1 envelope trimer. *Science* 342: 1477–1483
- Kallewaard NL, Corti D, Collins PJ, Neu U, McAuliffe JM, Benjamin E, Wachter-Rosati L, Palmer-Hill FJ, Yuan AQ, Walker PA, Vorlaender MK, Bianchi S, Guarino B, De Marco A, Vanzetta F, Agatic G, Foglierini M, Pinna D, Fernandez-Rodriguez B, Fruehwirth A et al (2016) Structure and function analysis of an antibody recognizing all influenza A subtypes. *Cell* 166: 596–608
- Lanzavecchia A (1985) Antigen-specific interaction between T and B cells. *Nature* 314: 537–539
- Lee J, Boutz DR, Chromikova V, Joyce MG, Vollmers C, Leung K, Horton AP, DeKosky BJ, Lee C-H, Lavinder JJ, Murrin EM, Chrysostomou C, Hoi KH, Tsybovsky Y, Thomas PV, Druz A, Zhang B, Zhang Y, Wang L, Kong W-P et al (2016) Molecular-level analysis of the serum antibody repertoire in young adults before and after seasonal influenza vaccination. *Nat Med* 22: 1456–1464
- Lillemeier BF, Pfeiffer JR, Surviladze Z, Wilson BS, Davis MM (2006) Plasma membrane-associated proteins are clustered into islands attached to the cytoskeleton. *Proc Natl Acad Sci USA* 103: 18992–18997
- Liu M, Yang G, Wiehe K, Nicely NI, Vandergriff NA, Rountree W, Bonsignori M, Alam SM, Gao J, Haynes BF, Kelsoe G (2015) Polyreactivity and autoreactivity among HIV-1 antibodies. *J Virol* 89: 784–798
- Manz J, Denis K, Witte O, Brinster R, Storb U (1988) Feedback inhibition of immunoglobulin gene rearrangement by membrane mu, but not by secreted mu heavy chains. *J Exp Med* 168: 1363–1381
- Maruyama T, Dougan SK, Truttmann MC, Bilate AM, Ingram JR, Ploegh HL (2015) Increasing the efficiency of precise genome editing with CRISPR-Cas9 by inhibition of nonhomologous end joining. *Nat Biotechnol* 33: 538–542
- Mattila PK, Feest C, Depoil D, Treanor B, Montaner B, Otipoby KL, Carter R, Justement LB, Bruckbauer A, Batista FD (2013) The actin and tetraspanin networks organize receptor nanoclusters to regulate B cell receptor-mediated signaling. *Immunity* 38: 461–474
- Nussenzweig MC, Shaw AC, Sinn E, Danner DB, Holmes KL, Morse HC, Leder P (1987) Allelic exclusion in transgenic mice that express the membrane form of immunoglobulin mu. *Science* 236: 816–819
- O'Connor BP, Vogel LA, Zhang W, Loo W, Shnyder D, Lind EF, Ratliff M, Noelle RJ, Erickson LD (2006) Imprinting the fate of antigen-reactive B cells through the affinity of the B cell receptor. *J Immunol* 177: 7723–7732
- Oji A, Noda T, Fujihara Y, Miyata H, Kim YJ, Muto M, Nozawa K, Matsumura T, Isotani A, Ikawa M (2016) CRISPR/Cas9 mediated genome editing in ES cells and its application for chimeric analysis in mice. *Sci Rep* 6: 31666
- Okada T, Miller MJ, Parker I, Krummel MF, Neighbors M, Hartley SB, O'Garra A, Cahalan MD, Cyster JG (2005) Antigen-engaged B cells undergo chemotaxis toward the T zone and form motile conjugates with helper T cells. *PLoS Biol* 3: e150

- Pappas L, Foglierini M, Piccoli L, Kallewaard NL, Turrini F, Silacci C, Fernandez-Rodriguez B, Agatic G, Giacchetto-Sasselli I, Pellicciotta G, Sallusto F, Zhu Q, Vicenzi E, Corti D, Lanzavecchia A (2014) Rapid development of broadly influenza neutralizing antibodies through redundant mutations. *Nature* 516: 418–422
- Paus D, Phan TG, Chan TD, Gardam S, Basten A, Brink R (2006) Antigen recognition strength regulates the choice between extrafollicular plasma cell and germinal center B cell differentiation. *J Exp Med* 203: 1081–1091
- Pelanda R, Schwers S, Sonoda E, Torres RM, Nemazee D, Rajewsky K (1997) Receptor editing in a transgenic mouse model: site, efficiency, and role in B cell tolerance and antibody diversification. *Immunity* 7: 765–775
- Pereira JP, Kelly LM, Xu Y, Cyster JG (2009) EB12 mediates B cell segregation between the outer and centre follicle. *Nature* 460: 1122–1126
- Pewzner-Jung Y, Friedmann D, Sonoda E, Jung S, Rajewsky K, Eilat D (1998) B cell deletion, anergy, and receptor editing in “knock in” mice targeted with a germline-encoded or somatically mutated anti-DNA heavy chain. *J Immunol* 161: 4634–4645
- Pierce SK, Liu W (2010) The tipping points in the initiation of B cell signalling: how small changes make big differences. *Nat Rev Immunol* 10: 767–777
- Qi H, Cannons JL, Klauschen F, Schwartzberg PL, Germain RN (2008) SAP-controlled T-B cell interactions underlie germinal centre formation. *Nature* 455: 764–769
- Quadros RM, Miura H, Harms DW, Akatsuka H, Sato T, Aida T, Redder R, Richardson GP, Inagaki Y, Sakai D, Buckley SM, Seshacharyulu P, Batra SK, Behlke MA, Zeiner SA, Jacobi AM, Izu Y, Thoreson WB, Urness LD, Mansour SL et al (2017) Easi-CRISPR: a robust method for one-step generation of mice carrying conditional and insertion alleles using long ssDNA donors and CRISPR ribonucleoproteins. *Genome Biol* 18: 92
- Ran FA, Hsu PD, Wright J, Agarwala V, Scott DA, Zhang F (2013) Genome engineering using the CRISPR-Cas9 system. *Nat Protoc* 8: 2281–2308
- Sanders RW, van Gils MJ, Derking R, Sok D, Ketas TJ, Burger JA, Ozorowski G, Cupo A, Simonich C, Goo L, Arendt H, Kim HJ, Lee JH, Pugach P, Williams M, Debnath G, Moldt B, van Breemen MJ, Isik G, Medina-Ramírez M et al (2015) HIV-1 vaccines. HIV-1 neutralizing antibodies induced by native-like envelope trimers. *Science* 349: aac4223
- Schwickert TA, Victora GD, Fooksman DR, Kamphorst AO, Mugnier MR, Gitlin AD, Dustin ML, Nussenzweig MC (2011) A dynamic T cell-limited checkpoint regulates affinity-dependent B cell entry into the germinal center. *J Exp Med* 208: 1243–1252
- Shih T-AY, Meffre E, Roederer M, Nussenzweig MC (2002) Role of BCR affinity in T cell dependent antibody responses *in vivo*. *Nat Immunol* 3: 570–575
- Soriano P (1999) Generalized lacZ expression with the ROSA26 Cre reporter strain. *Nat Genet* 21: 70–71
- Spillane KM, Tolar P (2017) B cell antigen extraction is regulated by physical properties of antigen-presenting cells. *J Cell Biol* 216: 217–230
- Steichen JM, Kulp DW, Tokatlian T, Escolano A, Dosenovic P, Stanfield RL, McCoy LE, Ozorowski G, Hu X, Kalyuzhnyi O, Briney B, Schiffrer T, Garces F, Freund NT, Gitlin AD, Menis S, Georgeson E, Kubitz M, Adachi Y, Jones M et al (2016) HIV vaccine design to target germline precursors of glycan-dependent broadly neutralizing antibodies. *Immunity* 45: 483–496
- Taki S, Meiering M, Rajewsky K (1993) Targeted insertion of a variable region gene into the immunoglobulin heavy chain locus. *Science* 262: 1268–1271
- Taylor JJ, Pape KA, Jenkins MK (2012) A germinal center-independent pathway generates unswitched memory B cells early in the primary response. *J Exp Med* 209: 597–606
- Tian M, Cheng C, Chen X, Duan H, Cheng H-L, Dao M, Sheng Z, Kimble M, Wang L, Lin S, Schmidt SD, Du Z, Joyce MG, Chen Y, DeKosky BJ, Chen Y, Normandin E, Cantor E, Chen RE, Doria-Rose NA et al (2016) Induction of HIV neutralizing antibody lineages in mice with diverse precursor repertoires. *Cell* 166: 1471–1484.e18
- Tolar P, Spillane KM (2014) Force generation in B-cell synapses: mechanisms coupling B-cell receptor binding to antigen internalization and affinity discrimination. *Adv Immunol* 123: 69–100
- Treanor B, Depoil D, Gonzalez-Granja A, Barral P, Weber M, Dushek O, Bruckbauer A, Batista FD (2010) The membrane skeleton controls diffusion dynamics and signaling through the B cell receptor. *Immunity* 32: 187–199
- Treanor B, Depoil D, Bruckbauer A, Batista FD (2011) Dynamic cortical actin remodeling by ERM proteins controls BCR microcluster organization and integrity. *J Exp Med* 208: 1055–1068
- Verkoczy L, Diaz M, Holl TM, Ouyang Y-B, Bouton-Verville H, Alam SM, Liao H-X, Kelsoe G, Haynes BF (2010) Autoreactivity in an HIV-1 broadly reactive neutralizing antibody variable region heavy chain induces immunologic tolerance. *Proc Natl Acad Sci USA* 107: 181–186
- Verkoczy L, Chen Y, Bouton-Verville H, Zhang J, Diaz M, Hutchinson J, Ouyang Y-B, Alam SM, Holl TM, Hwang K-K, Kelsoe G, Haynes BF (2011) Rescue of HIV-1 broad neutralizing antibody-expressing B cells in 2F5 VH x VL knockin mice reveals multiple tolerance controls. *J Immunol* 187: 3785–3797
- Verkoczy L, Alt FW, Tian M (2017) Human Ig knockin mice to study the development and regulation of HIV-1 broadly neutralizing antibodies. *Immunol Rev* 275: 89–107
- Weaver D, Costantini F, Imanishi-Kari T, Baltimore D (1985) A transgenic immunoglobulin mu gene prevents rearrangement of endogenous genes. *Cell* 42: 117–127
- Wienands J, Larbolette O, Reth M (1996) Evidence for a preformed transducer complex organized by the B cell antigen receptor. *Proc Natl Acad Sci USA* 93: 7865–7870
- Yang J, Reth M (2010) Oligomeric organization of the B-cell antigen receptor on resting cells. *Nature* 467: 465–469
- Yang H, Wang H, Jaenisch R (2014) Generating genetically modified mice using CRISPR/Cas-mediated genome engineering. *Nat Protoc* 9: 1956–1968